

Ultra High Energy Cosmic Rays Spectra in Top-Down models

R. Aloisio^a *, V. Berezhinsky^a and M. Kachelrieß^b

^aINFN - Laboratori Nazionali del Gran Sasso, I-67010 Assergi (AQ), Italy

^bMax-Planck-Institut für Physik (Werner-Heisenberg-Institut), D-80805 München, Germany

In this work we present a detailed computation of the spectra of UHECR in the top-down scenario. We compare the spectra of hadrons obtained by two different methods in QCD and supersymmetric (SUSY) QCD with large primary energies \sqrt{s} up to 10^{16} GeV. The two methods discussed are a Monte Carlo (MC) simulation and the evolution of the hadron fragmentation functions as described by the Dokshitzer-Gribov-Lipatov-Altarelli-Parisi (DGLAP) equations. The hadron spectra obtained by the two methods agree fairly well in the interesting energy range $10^{-5}M_X < E < 0.3M_X$ (M_X is the energy scale of the process $M_X \geq 10^{12}$ GeV). We have also computed the spectra of photons, neutrinos and nucleons obtaining a good agreement with other published results. The consistency of the spectra computed by different methods allows us to consider the spectral shape as a signature of the production model for UHECR, such as the decay of super heavy relic particles or topological defects.

1. Introduction

Ultra High Energy Cosmic Rays (UHECRs) are still an open problem in astro-particle physics. The 11 Akeno Grand Air Shower Array (AGASA) events with energy larger than 10^{20} eV [1] contradict the expected suppression of the UHECR spectrum due to the interaction with the Cosmic Microwave Background (CMB) radiation, the GZK cut-off [2]. On the other hand the HiRes data seems to be consistent with the GZK cut-off picture [1]. If the UHECR primaries are protons and if they propagate rectilinearly, as the claimed correlation with BL-Lacs at energy $4 - 8 \times 10^{19}$ eV implies, than their sources must be seen in the direction of the highest energies events with energies up to $2 - 3 \times 10^{20}$ eV detected by HiRes, Fly's Eye and AGASA [1]. At these energies the proton attenuation length is only about 20 – 30 Mpc and no counterparts in any frequency band was observed in the direction of these UHECR events. This is a strong indication that CR particles with energies larger than 10^{20} eV may have a different origin from those with lower energies.

Another important point of this discussion is

related to the low energy part of the CR spectrum, there are, infact, strong evidences that these CR with energies $1 \times 10^{18} \text{eV} \leq E \leq 7 - 8 \times 10^{19} \text{eV}$ are extragalactic protons, most probably from Active Galactic Nuclei (AGNs). This statement is based on some robust experimental and theoretical evidences: (i) extensive air shower (EAS) data confirm protons as primaries, (ii) the dip seen with great accuracy in the data of AGASA, HiRes, Fly's Eye and Yakutsk, is a strong signature of the propagation of UHE protons in the extragalactic space, (iii) the beginning of the GZK cut-off seen in the spectra of AGASA and HiRes. Excluding the correlation of UHECR with BL Lacs from the analysis becomes also possible the propagation of protons in very strong magnetic fields. Nevertheless, also in this case, the lack of a nearby source in the direction of the highest energy events (e.g. at $E \sim 3 \times 10^{20}$ eV) remains a problem. In fact, for very strong field strengths $B \sim 1$ nG: the deflection angle, $\theta \sim l_{\text{att}}/r_H = 3.7^\circ B_{\text{nG}}$ given by the attenuation length l_{att} and the Larmor radius r_H , is small and sources should be seen.

Many ideas have been put forward aiming to explain the observed superGZK ($E \gtrsim (6 - 8) \times 10^{19}$ eV) events: strongly interacting neutrinos

*Talk presented by R. Aloisio

and new light hadrons as unabsorbed signal carriers, Z -bursts, Lorentz-invariance violation, Topological Defects (TD) and Superheavy Dark Matter (SHDM) (see [3] for reviews). The two last models listed above, that represent the most promising top-down models, share a common feature: UHE particles are produced in the decay of superheavy (SH) particles or in their annihilation. In the case of TD they are unstable and in the case of SHDM long-lived particles. We shall call them collectively X particles. Annihilation takes place in the case of monopolonia, necklaces [4] and SHDM particles within some special models. From the point of view of elementary particle physics all these processes proceed in a way similar to e^+e^- annihilation into hadrons: two or more off-mass-shell quarks and gluons are produced and they initiate QCD cascades. Finally the partons are hadronized at the confinement radius. Most of the hadrons in the final state are pions and thus the typical prediction of all these models is the dominance of photons at the highest energies $E \gtrsim (6 - 8) \times 10^{19}$ eV. Let us now concentrate our attention to the computation of the UHECR spectrum produced in the decay of X particles.

The spectrum of hadrons produced in the decay/annihilation of X particles is another signature of models with superheavy X particles. The mass of the decaying particle, M_X , or the energy of annihilation \sqrt{s} , is in the range $10^{13} - 10^{16}$ GeV. The existing QCD MC codes become numerically unstable at much smaller energies, e.g., at $M_X \sim 10^7$ GeV. Moreover, the computing time increases rapidly going to larger energies. In this work we will review our results obtained, in the computation of the top-down spectrum of UHECR, using two different computational techniques: one based on a MC computation scheme [5] and the other based on the DGLAP evolution equations [5]. In both cases SUSY is included in the computation. Monte Carlo simulations are the most physical approach for high energy calculations which allow to incorporate many important physical features as the presence of SUSY partons in the cascade and coherent branching. The perturbative part of our MC simulation scheme is similar to other existing MC

codes it also includes in a standard way SUSY and hence is reliable. For the non-perturbative hadronization part an original phenomenological approach is used in Ref. [5]. The fragmentation of a parton i into an hadron h is expressed through perturbative fragmentation function of partons $D_i^j(x, M_X)$, that represents the probability of fragmentation of a parton i into a parton j with momentum fraction $x = 2p/M_X$, convoluted with the hadronization functions $f_j^h(x, Q_0)$ at scale Q_0 , that is understood as the fragmentation function of the parton i into the hadron h at the hadronization scale $Q_0 \simeq 1.4$ GeV [5]. To obtain the fragmentation functions of hadrons one has:

$$D_i^h(x, M_X) = \sum_{j=q,g} \int_x^1 \frac{dz}{z} D_i^j\left(\frac{x}{z}, M_X\right) f_j^h(z, Q_0) \quad (1)$$

where the hadronization functions do not depend on the scale M_X . This important property of hadronization functions allows us to calculate $f_i^h(x, Q_0)$ from available LEP data, $D_i^h(x, M_X)$ at the scale $M_X = M_Z$, and then to use it for the calculation of fragmentation functions $D_i^h(x, M_X)$ at any arbitrary scale M_X . Our approach reduces the computing time compared to usual MC simulations and allows a fast calculation of hadron spectra for large M_X up to M_{GUT} .

The perturbative part of the MC simulation in Ref. [5] includes standard features such as angular ordering, which provides the coherent branching and the correct Sudakov form factors, as well as SUSY partons. Taking into account SUSY partons results only in small corrections to the production of hadrons, and therefore a simplified spectrum of SUSY masses works with good accuracy. The weak influence of supersymmetry is explained by the decay of SUSY partons, when the scale of the perturbative cascade reaches the SUSY scale $Q_{\text{SUSY}}^2 \sim 1 \text{ TeV}^2$. Most of the energy of SUSY partons remains in the cascade in the form of energy of ordinary partons, left after the decay of SUSY partons. The qualitatively new effect caused by supersymmetry is the effective production of the Lightest Supersymmetric Particles (LSP), which could be neutralinos or gluinos. The fragmentation functions $D_i^h(x, M_X)$ at a high scale M_X can be calculated also evol-

ing them from a low scale, e.g. $M_X = M_Z$, where they are known experimentally or with great accuracy using the MC scheme. This evolution is described by the Dokshitzer-Gribov-Lipatov-Altarelli-Parisi (DGLAP) equation [6] which can be written as

$$\partial_t D_i^h = \sum_j \frac{\alpha_s(t)}{2\pi} P_{ij}(z) \otimes D_j^h(x/z, t), \quad (2)$$

where $t = \ln(s/s_0)$ is the scale, \otimes denotes the convolution $f \otimes g = \int_z^1 dx/x f(x)g(x/z)$, and P_{ij} is the splitting function which describes the emission of parton j by parton i . Apart from the experimentally rather well determined quark fragmentation function $D_q^h(x, M_Z)$, also the gluon fragmentation function $D_g^h(x, M_Z)$ is needed for the evolution of Eq. (2). The gluon FF can be taken either from MC simulations or from fits to experimental data, in particular to the longitudinal polarized e^+e^- annihilation cross-section and three-jet events.

The first application of the DGLAP method for the calculation of hadron spectra from decaying superheavy particles has been made in Refs. [7]. The most detailed calculations have been performed by Barbot and Drees [7], where more than 30 different particles were allowed to be cascading and the mass spectrum of the SUSY particles was taken into account. Although at M_Z , which is normally the initial scale in the DGLAP method, the fragmentation functions for supersymmetric partons are identically zero, they can be calculated at larger scales t : SUSY partons are produced above their mass threshold, when their splitting functions are included in Eq. (2). In [5] we proved that this method is correct. Also, the LSP spectrum can be computed within the DGLAP approach [7].

In this paper we shall study the agreement of the two methods: MC and DGLAP equations for the calculation of spectra produced in the decay or annihilation of superheavy particles. We shall also compare the results obtained by different groups comparing the calculated spectra with recent ones measured by UHECR experiments.

The paper is organized as follows: in Section 2 we will compare the two computation schemes

described, referring the reader to our paper [5] for more details. Photon, neutrino and proton spectra, needed for UHECR calculations, are computed in Section 3 and compared with the spectra obtained in [7]. In Section 4 we will discuss the consequences of our results for models of SHDM and TD in the explanation of the UHECR spectrum. We will conclude in section 5.

2. MC and DGLAP comparison

In this Section we shall compare the hadron spectra computed by the two methods discussed above, MC and DGLAP. In Figure 1 we plot the FFs $D_i^h(x, M_X)$ calculated by SUSY MC and SUSY DGLAP methods for $M_X = 1 \times 10^{16}$ GeV and $i = q$. In the DGLAP method the SUSY FFs have been evolved from the ones obtained with the SUSY MC at the scale $\sqrt{s} = 10M_{\text{SUSY}} \approx 10$ TeV. One can see the good agreement between DGLAP (solid curve) and MC (dotted curve). This good agreement holds also for other (lower) scales M_X and for other initial partons, e.g. gluon, squark or gluino. One can see that the MC and DGLAP spectra slightly differ at very low x and have a more pronounced disagreement at large values of x . The discrepancy at low x is due to coherent branching, that is included in the MC scheme while it cannot be embedded in the DGLAP one. At large x , the calculations by both methods suffer from uncertainties, particularly the MC simulation. In this region the results are sensitive to the details of the hadronization scheme (see, e.g., the problem of HERWIG [7] with the overproduction of protons at large x). When one does not have the initial SUSY FFs from a MC simulation, the question arises how to proceed. As was first suggested by Rubin [7], the initial FFs can be taken as the ones for ordinary QCD at the low scale $\sqrt{s} = M_Z$, while the production of SUSY partons is included in the splitting functions assuming threshold behavior at $M_{\text{SUSY}} \sim 1$ TeV. We can check this assumption computing the SUSY FF in both ways. In Figure 1 we present the SUSY FFs $D_i^h(x, M_X)$ for $i = q$ and $M_X = 1 \times 10^{16}$ GeV, evolved from the initial scale $\sqrt{s} = M_Z$ (dashed curve). The good agreement between the two DGLAP curves

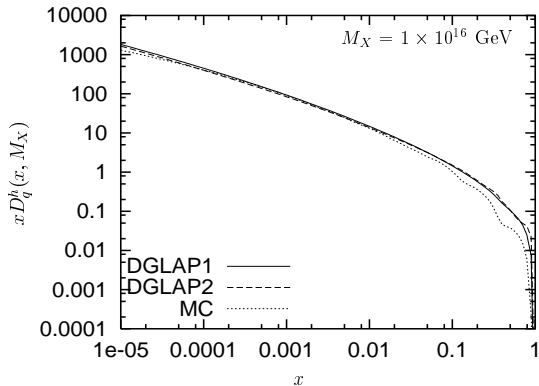


Figure 1. Comparison of SUSY DGLAP and SUSY MC fragmentation functions for $M_X = 1 \times 10^{16}$ GeV with quark as a primary parton. SUSY DGLAP FFs are calculated for 10 TeV as the starting scale (solid line) and for M_Z (broken line). SUSY MC FF is shown by dotted line.

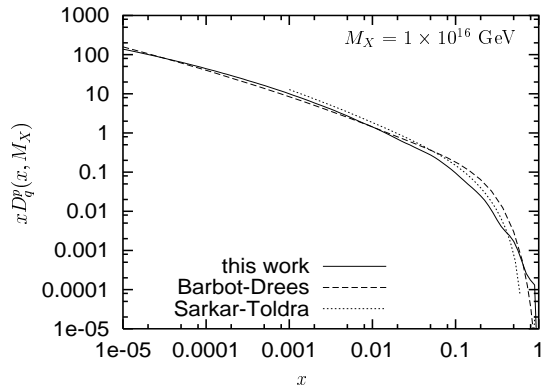


Figure 2. Comparison of nucleon spectra from present work computed with DGLAP equation (solid line), from Barbot & Drees [7] (dashed line) and Sarkar & Toldrà [7] (dotted line). All three calculations are performed with quark as initial parton for $M_X = 1 \times 10^{16}$ GeV.

proves the validity of the assumption made.

3. Photon, neutrino and nucleon spectra

The spectra of photons, neutrinos and nucleons produced by the decay of superheavy particles are of practical interest in high energy astrophysics. These spectra $D_i^a(x, M_X)$ with $a = \gamma, \nu, N$ can be also considered as FFs. Because the dependence on the type i of the primary parton is weak, we shall omit the index i from now on, keeping a as subscript.

Till now we concentrated our discussion on the total number of hadrons ($a = h$) described by the FF $D_h(x, M_X)$, but in fact we have performed similar calculations separately for charged pions and protons+antiprotons. The procedure of the calculations is identical to that already described for the DGLAP and MC computation schemes. For charged pions and protons+antiprotons we used experimental data from Refs. [8]. Below we shall present results of our SUSY MC simulations in terms of FFs for all pions D_π , all nucleons D_N and all hadrons D_h . We introduce the ratios $\varepsilon_N(x)$ and $\varepsilon_\pi(x)$ as: $D_N(x) = \varepsilon_N(x)D_h(x)$

and $D_\pi(x) = \varepsilon_\pi(x)D_h(x)$. The spectra of pions and nucleons at large M_X have approximately the same shape as the hadron spectra, and one can use in this case $\varepsilon_\pi = 0.73 \pm 0.03$ and $\varepsilon_N = 0.12 \pm 0.02$ [5], taking into account the errors in the experimental data [8]. We can calculate now the spectra of photons and neutrinos produced by the decays of pions neglecting the small contribution (0.15 ± 0.04) of K , D , Λ and other particles. Including these particles affects stronger neutrinos than nucleons and photons, which are the main topic of this Section.

The normalized photon and neutrino spectrum from the decay of one X particle at rest can be computed using the pion and nucleon FF following the recipe given in [5]. We shall compare our photon spectra with those calculated by the DGLAP method in [7]. The photon spectrum is most interesting to compare, because it is straightforwardly related to the hadron spectrum which is the basic physical quantity. Moreover, the photon spectrum is the dominant component of radiation produced by superheavy particles.

To be precise, we compare the FF $D_q^{\gamma, N, \nu}(x, M_X)$ at $M_X = 1 \times 10^{16}$ GeV. Figure 2,

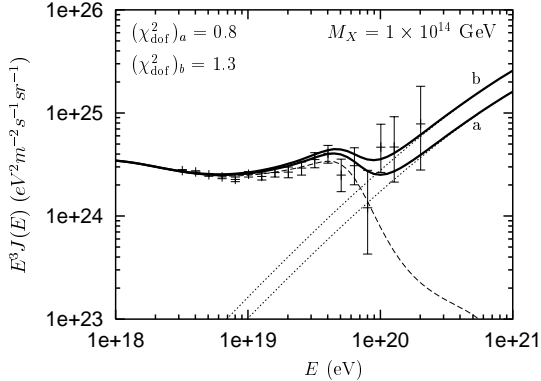


Figure 3. Comparison of SHDM prediction with the AGASA data. The calculated spectrum of SHDM photons is shown by dotted curves for two different normalizations. The dashed curve gives the spectrum of extragalactic protons from uniformly distributed astrophysical sources. The sum of these two spectra is shown by the thick curves. The χ^2 values are given of the comparison of these curves with experimental data for $E \geq 4 \times 10^{19}$ eV.

that is referred to nucleons, demonstrates good agreement between our spectrum and those from [7] at $x \leq 0.3$. As it was mentioned above, the disagreement at large x is not surprising. Apart from $D_q^h(x, M_Z)$ taken directly from the experiments, both calculations use the much more uncertain $D_g^h(x, Q^2)$. In our case, $D_g^h(x, Q^2)$ is taken from our MC simulation [5], in the case of Barbot & Drees in [7] from the fit performed in Ref. [9]. In both cases, rather large uncertainties exist at large x [9]. The agreement between the three curves as presented in Figure 2 is good. The same conclusion holds for the comparison of photons and neutrino spectra [5].

4. UHECR from SuperHeavy particles and Topological Defects

As follows from the previous section, the accuracy of spectrum calculations has reached such a level that one can consider the spectral shape as a

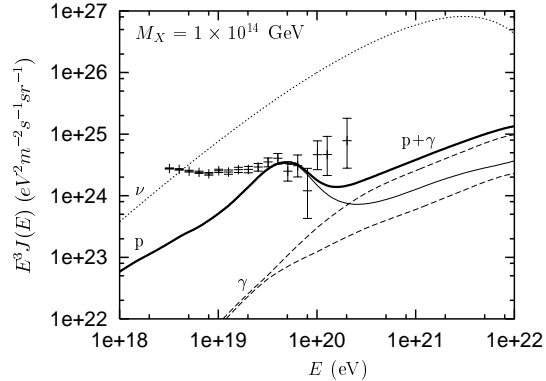


Figure 4. Diffuse spectra from necklaces. The upper curve shows neutrino flux, the middle - proton flux, and two lower curves - photon fluxes for two cases of absorption. The thick continuous curve gives the sum of the proton and higher photon flux.

signature of the model. The predicted spectrum is approximately $\propto dE/E^{1.9}$ in the region of x at interest. Another interesting feature of these new calculations is a decrease of the ratio of photons to nucleons, γ/N , in the generation spectrum. At $x \sim 1 \times 10^{-3}$ this ratio is characterized by a value of 2 – 3 only [5]. The decrease of the γ/N ratio is caused by a decrease of the number of pions in the new calculations. This result has an important impact for SHDM and topological defect models because the fraction of nucleons in the primary radiation increases. However, in both models photons dominate (i.e. their fraction becomes $\gtrsim 50\%$) at $E \gtrsim (7-8) \times 10^{19}$ eV. In this Section we shall consider: UHECR from superheavy dark matter (SHDM) [10] and topological defects (TD) [11]. Production of SHDM particles naturally occurs in the time-varying gravitational field of the expanding universe at the post-inflationary stage. The relic density of these particles is mainly determined (at fixed reheating temperature and inflaton mass) by their mass M_X . The range of practical interest is $(3-10) \times 10^{13}$ GeV, at larger masses the SHDM is a subdominant component of the DM. SHDM is accumulated in the Galac-

tic halo with the overdensity $\delta = \frac{\rho_X^{\text{halo}}}{\rho_X^{\text{extr}}} = \frac{\bar{\rho}_{\text{DM}}^{\text{halo}}}{\Omega_{\text{CDM}}\rho_{\text{cr}}}$, where $\bar{\rho}_{\text{DM}}^{\text{halo}} \approx 0.3 \text{ GeV}/\text{cm}^3$, $\rho_{\text{cr}} = 1.88 \times 10^{-29} h^2 \text{ g}/\text{cm}^3$ and $\Omega_{\text{CDM}} h^2 = 0.135$ [12]. With these numbers, $\delta \approx 2.1 \times 10^5$. Because of this large overdensity, UHECRs from SHDM have no GZK cutoff.

Clumpiness of SHDM in the halo can provide the observed small-angle clustering. The ratio $r_X = \Omega_X(t_0/\tau_X)$ of relic abundance Ω_X and lifetime τ_X of the X particle is fixed by the observed UHECR flux as $r_X \sim 10^{-11}$. The numerical value of r_X is theoretically calculable as soon as a specific particle physics and cosmological model is fixed. In the most interesting case of gravitational production of X particles, their present abundance is determined by their mass M_X and the reheating temperature T_R . Choosing a specific particle physics model one can fix also the lifetime of the X particle. There exist many models in which SH particles can be quasi-stable with lifetime $\tau_X \gg 10^{10} \text{ yr}$. The measurement of the UHECR flux, and thereby of r_X , selects from the three-dimensional parameter space (M_X, T_R, τ_X) a two-dimensional subspace compatible with the SHDM hypothesis.

In Figure 3 we have performed a fit to the AGASA data using the photon flux from the SHDM model and the proton flux from uniformly distributed astrophysical sources. For the latter we have used the non-evolutionary model. The photon flux is normalized to provide the best fit to the AGASA data at $E \geq 4 \times 10^{19} \text{ eV}$. The fits are shown in Figure 3 with $\chi^2/\text{d.o.f.}$ indicated there. *One can see from the fits in Figure 3, that the SHDM model with the new spectra can explain only the excess of AGASA events at $E \gtrsim 1 \times 10^{20} \text{ eV}$: depending on the SHDM spectrum normalization and the details of the calculations for the extragalactic protons, the flux from SHDM decays becomes dominant only above $(6 - 8) \times 10^{19} \text{ eV}$.*

Topological Defects (for review see [3] and reference therein) can naturally produce UHE particles. The following TD have been discussed as potential sources of UHE particles: superconducting strings, ordinary strings, monopolonium (bound monopole-antimonopole pair), monopolo-

nia (monopole-antimonopole pairs connected by a string), networks of monopoles connected by strings, vortons and necklaces (see Ref. [3] for a review and references). Monopolonia and vortons are clustering in the Galactic halo and their observational signatures for UHECR are identical to SHDM. However the friction of monopolonia in cosmic plasma results in monopolonium lifetime much shorter than the age of the universe. Of all other TD which are not clustering in the Galactic halo, the most favorable for UHECR are *necklaces*. Their main phenomenological advantage is a small separation which ensures the arrival of highest energy particles to our Galaxy. We shall calculate here the flux of UHECR from necklaces.

Necklaces are hybrid TD produced in the symmetry breaking pattern $G \rightarrow H \times U(1) \rightarrow H \times Z_2$. At the first symmetry breaking monopoles are produced, at the second one each (anti-)monopole get attached to two strings. This system resembles ordinary cosmic strings with monopoles playing the role of beads. Necklaces exist as the long strings and loops. The symmetry breaking scales of the two phase transitions, η_m and η_s , are the main parameters of the necklaces. They determine the monopole mass, $m \sim 4\pi\eta_m/e$, and the mass of the string per unit length $\mu \sim 2\pi\eta_s^2$. The evolution of necklaces is governed by the ratio $r \sim m/\mu d$, where d is the average separation of a monopole and antimonopole along the string. As it is argued in Ref. [4], necklaces evolve towards configuration with $r \gg 1$. Monopoles and antimonopoles trapped in the necklaces inevitably annihilate in the end, producing heavy Higgs and gauge bosons (X particles) and then hadrons. The rate of X particles production in the universe can be estimated as [4] $\dot{n}_X \sim \frac{r^2 \mu}{t^3 M_X}$, where t is the cosmological time.

The photons and electrons from pion decays initiate e-m cascades and the cascade energy density can be calculated as $\omega_{\text{cas}} = \frac{1}{2} f_\pi r^2 \mu \int_0^{t_0} \frac{dt}{t^3} \frac{1}{(1+z)^4} = \frac{3}{4} f_\pi r^2 \frac{\mu}{t_0^2}$, where z is the redshift and $f_\pi \sim 1$ is the fraction of the total energy release transferred to the cascade. The parameters of the necklace model for UHECR

are restricted by the EGRET observations [13] of the diffuse gamma-ray flux. This flux is produced by UHE electrons and photons from necklaces due to e-m cascades initiated in collisions with CMB photons. In the range of the EGRET observations, $10^2 - 10^5$ MeV, the predicted spectrum is $\propto E^{-\alpha}$ with $\alpha = 2$ [14]. The EGRET observations determined the spectral index as $\alpha = 2.10 \pm 0.03$ and the energy density of radiation as $\omega_{\text{obs}} \approx 4 \times 10^{-6}$ eV/cm³. The cascade limit consists in the bound $\omega_{\text{cas}} \leq \omega_{\text{obs}}$.

According to the recent calculations, the Galactic contribution of gamma rays to the EGRET observations is larger than estimated earlier, and the extragalactic gamma-ray spectrum is not described by a power-law with $\alpha = 2.1$. In this case, the limit on the cascade radiation with $\alpha = 2$ is more restrictive and is given by $\omega_{\text{cas}} \leq 2 \times 10^{-6}$ eV/cm³; we shall use this limit in further estimates. Using ω_{cas} with $f_\pi = 1$ and $t_0 = 13.7$ Gyr [12] we obtain from the limit on the cascade radiation $r^2\mu \leq 8.9 \times 10^{27}$ GeV².

The important and unique feature of this TD is the small separation D between necklaces. It is given by $D \sim r^{-1/2}t_0$ [4]. Since $r^2\mu$ is limited by e-m cascade radiation we can obtain a lower limit on the separation between necklaces as $D \sim \left(\frac{3f_\pi\mu}{4t_0^2\omega_{\text{cas}}}\right)^{1/4} t_0 > 10(\mu/10^6 \text{ GeV}^2)^{1/4}$ kpc, this small distance is a unique property of necklaces allowing the unabsorbed arrival of particles with the highest energies. The fluxes of UHECR from necklaces are shown in Figure 4. We used in the calculations $r^2\mu = 4.7 \times 10^{27}$ GeV² which corresponds to $\omega_{\text{cas}} = 1.1 \times 10^{-6}$ eV/cm³, i.e. twice less than allowed by the bound on ω_{cas} . The mass of the X particles produced by monopole-antimonopole annihilations is taken as $M_X = 1 \times 10^{14}$ GeV. From Figure 4 one can see that the necklace model for UHECR can explain only the highest energy part of the spectrum, with the AGASA excess somewhat above the prediction. This is the direct consequence of the new spectrum of particles in X decays obtained in this work. Thus UHE particles from necklaces can serve only as an additional component in the observed UHECR flux.

5. Conclusions

In this paper we have compared the MC and DGLAP methods for the calculation of hadron spectra produced by the decay (or annihilation) of superheavy X particles with masses up to $M_{\text{GUT}} \sim 1 \times 10^{16}$ GeV. We found an excellent agreement of these two methods. The calculations have been performed both for ordinary QCD and SUSY QCD. The inclusion of SUSY partons in the development of the cascade results only in small corrections, and it justifies our computation scheme with a single mass scale M_{SUSY} [5].

In comparison to the DGLAP method, the MC simulation has the advantage of including coherent branching. It allows reliable calculations at very small x . The Gaussian peak, the signature of the QCD spectrum, cannot be obtained using the DGLAP equations. We have calculated the all-hadron spectra, as well as spectra of charged pions and nucleons, using the DGLAP equations.

Our nucleon spectrum agrees well with that of Refs. [7]. We compared also our spectrum of photons with the calculations of Ref. [7]. The comparison of the photon spectra is interesting, because of physical reasons (photons can be observable particles), and because the photon spectra are connected directly with the hadron spectra. The spectra are in good agreement. We conclude that all calculations are in a good agreement especially in the most interesting low x regime and the predicted shape of the generation spectrum ($\propto dE/E^{1.9}$) can be considered as a signature of models with decaying (annihilating) superheavy particles.

The predicted spectrum of SHDM model cannot fit the observed UHECR spectrum at $1 \times 10^{18} \text{ eV} \leq E \leq (6 - 8) \times 10^{19} \text{ eV}$. Only events at $E \gtrsim (6 - 8) \times 10^{19} \text{ eV}$, and most notably the AGASA excess at these energies, can be explained in this model. The robust prediction of this model is photon dominance. In present calculations this excess diminishes to $\gamma/N \simeq 2-3$ [5]. According to the recent calculations the muon content of photon induced EAS at $E > 1 \times 10^{20} \text{ eV}$ is high, but lower by a factor 5 - 10 than in hadronic showers. The muon content of EAS at $E > 1 \times 10^{20} \text{ eV}$ has been recently measured in AGASA [1]. The mea-

sured value is the muon density at the distance 1000 m from the shower core, $\rho_\mu(1000)$. From 11 events at $E > 1 \times 10^{20}$ eV the muon density was measured in 6. In two of them with energies about 1×10^{20} eV, ρ_μ is almost twice higher than predicted for gamma-induced EAS. Taking into account the contribution of extragalactic protons at this energy, the ratio γ/p predicted by the SHDM model is 1.2 – 1.4. It is lower than the upper limit $\gamma/p \leq 2$ obtained by AGASA at $E = 3 \times 10^{19}$ eV on the basis of a much larger statistics. The muon content of the remaining 4 EAS marginally agrees with that predicted for gamma-induced showers. The contribution of extragalactic protons for these events is negligible, and the fraction of protons in the total flux can be estimated as $0.25 \leq p/\text{tot} \leq 0.33$. This fraction gives a considerable contribution to the probability of observing 4 showers with slightly increased muon content. Not excluding the SHDM model, the AGASA events give no evidence in favor of it.

The simultaneous observation of UHECR events in fluorescent light and with water Cherenkov detectors has a great potential to distinguish between photon and proton induced EAS. An anisotropy towards the direction of the Galactic Center is another signature of the SHDM model. Both kinds of informations from Auger [1] will be crucial for the SHDM model and other top-down scenarios. Topological defect models are another case when short-lived superheavy particle decays can produce UHECR. In Figure 4 the spectra from necklaces are presented. One can see that at $E \gtrsim 1 \times 10^{20}$ eV photons dominate, and the discussion in the previous paragraph applies here too. In contrast to previous calculations, the agreement with observations is worse: necklaces can explain only the highest energy part of the spectrum in Figure 4, with the AGASA excess somewhat above the prediction. In the other energy ranges, UHE particles from necklaces can provide only a subdominant component. Other TDs suffer even more problems.

REFERENCES

1. M. Takeda *et al.* [AGASA collaboration], astro-ph/0209422. N. Hayashida *et al.* [AGASA collaboration], Phys. Rev. Lett. **73**, 3491 (1994). K. Shinozaki *et al.* [AGASA collaboration], Astrophys. J. **571**, L 117 (2002). T. Abu-Zayyad *et al.* [HiRes collaboration], astro-ph/0208243. D.J. Bird *et al.* [Fly’s Eye collaboration], Ap.J. **424**, 491 (1994). J. Blümer *et al.* [Auger Collaboration], J. Phys. **G29** 867 (2003).
2. K. Greisen, Phys. Rev. Lett. **16**, 748 (1966); G.T. Zatsepin and V.A. Kuzmin, JETP Lett. **4**, 78 (1966) [Pisma Zh. Eksp. Teor. Fiz. **4**, 114 (1966)].
3. V.S. Berezinsky, Nucl. Phys. (Proc. Suppl) **B87**, 387 (2000). V.A. Kuzmin and I.I. Tkachev, Phys. Rep. **320**, 199 (1999).
4. V.S. Berezinsky and A. Vilenkin, Phys. Rev. Lett. **79**, 5202 (1997).
5. R. Aloisio, V. Berezinsky and M. Kachelrieß, Phys. Rev. **D69** 094023 (2004).
6. V.N. Gribov and L.N. Lipatov, Sov. J. Nucl. Phys. **15**, 438 (1972); Yu. L. Dokshitser, Sov. Phys. JETP **46**, 641 (1977). G. Altarelli and G. Parisi, Nucl. Phys. **B126**, 298 (1977).
7. N.A. Rubin, Thesis, Cavendish Laboratory, University of Cambridge (1999). S. Sarkar and R. Toldrà, Nucl. Phys. **B621**, 495 (2002). Z. Fodor and S.D. Katz, Phys. Rev. Lett. **86**, 3224 (2001). C. Barbot and M. Drees, Astropart. Phys. **20**, 5 (2003).
8. R. Itoh *et al.* [TOPAZ collaboration], Phys. Lett. **B345**, 335 (1995). D. Buskulic *et al.* [ALEPH collaboration], Z. Phys. **C66**, 355 (1995); P. Abreu *et al.* [DELPHI collaboration], *ibid* **C73**, 11 (1996); G. Alexander *et al.* [OPAL collaboration], *ibid* **72**, 191 (1996).
9. B. A. Kniehl, G. Krämer and B. Pötter, Nucl. Phys. **B 582**, 514 (2000).
10. V. Berezinsky, M. Kachelrieß and A. Vilenkin, Phys. Rev. Lett. **79**, 4302 (1997). V.A. Kuzmin and V.A. Rubakov, Phys. At. Nucl. **61**, 1028 (1998).
11. C.T. Hill, D.N. Schramm and T.P. Walker, Phys. Rev. **D36**, 1007 (1987).
12. D.N. Spergel *et al.* [WMAP collaboration], astro-ph/0302209.
13. P. Sreekumar *et al.*, Ap.J., **494**, 523, (1998).
14. V.S. Berezinsky and A. Yu. Smirnov, Ap.Sp.Sci. **32**, 463, (1975),